The Impact of Preprocessing on Deep Representations for Iris Recognition on Unconstrained Environments

Luiz A. Zanlorensi[1], Eduardo Luz[2], Rayson Laroca[1], Alceu S. Britto Jr.[3], Luiz S. Oliveira[1] and David Menotti[1]

[1]Federal University of Paraná (UFPR)
[2]Federal University of Ouro Preto (UFOP)
[3]Pontifical Catholic University of Paraná (PUC-PR)

SIBGRAPI, 2018

UFPR

Visão Robótica Imagem

Eye regions

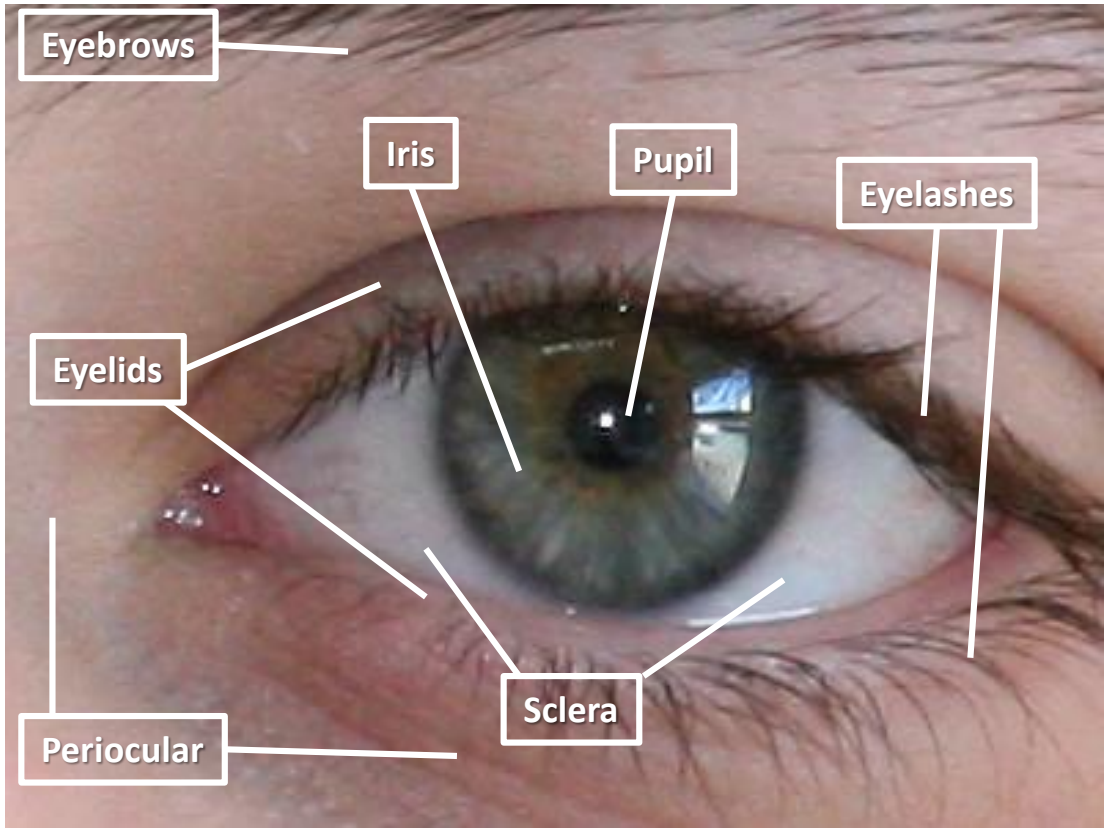

Image from the NICE.II dataset [Proença and Alexandre, 2012].

Iris recognition steps:

1. Image acquisition;
2. Preprocessing:

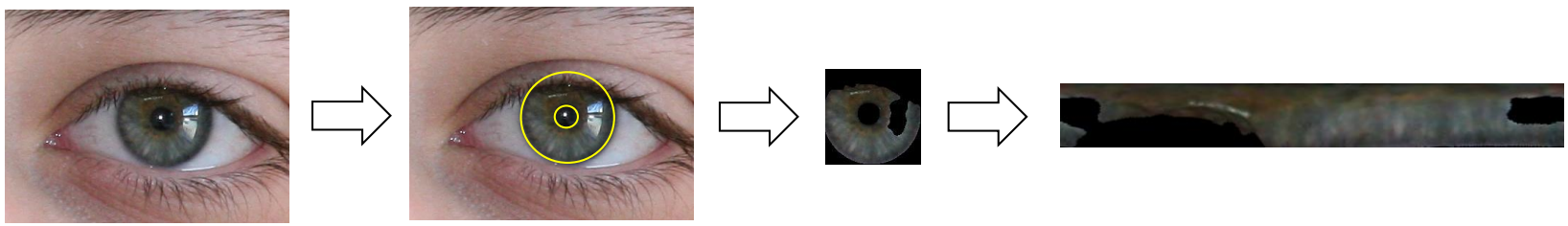

(a) (b) (c) (d)

3. Feature extraction;
4. Matching;

Image Preprocessing

Segmentation: winner of the NICE.I contest [Tan et al., 2010].

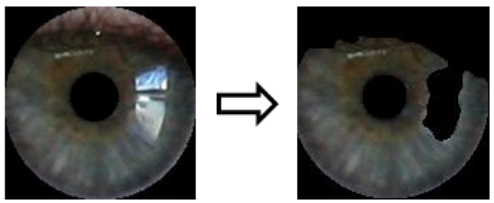

Normalization: rubber sheet model [Daugman, 1993].

Image Preprocessing

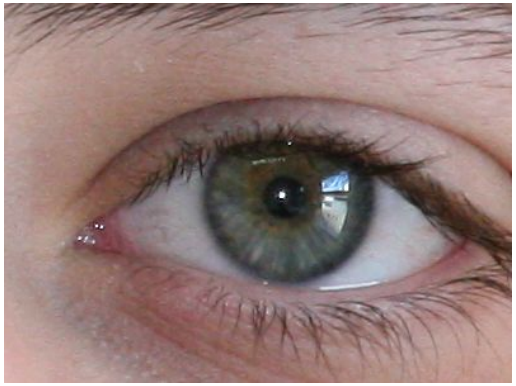

Original Image

Non-Segmented

Segmented

Recognition System

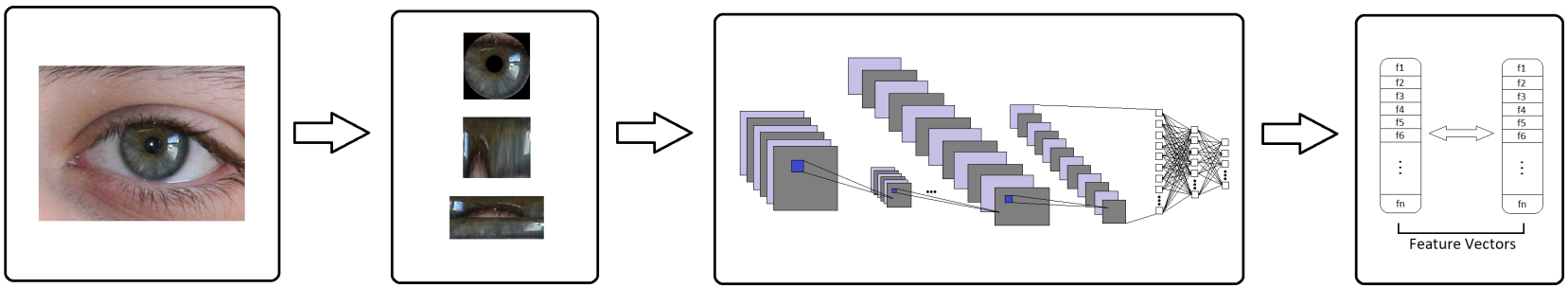

Original Image | Preprocessing | Deep features extraction | Matching

CNN models

- VGG16: convolution, activation (ReLu), pooling and fully connected layers.
- ResNet-50: residual information.
- Architecture modification: fully-connected layer with 256 neurons.

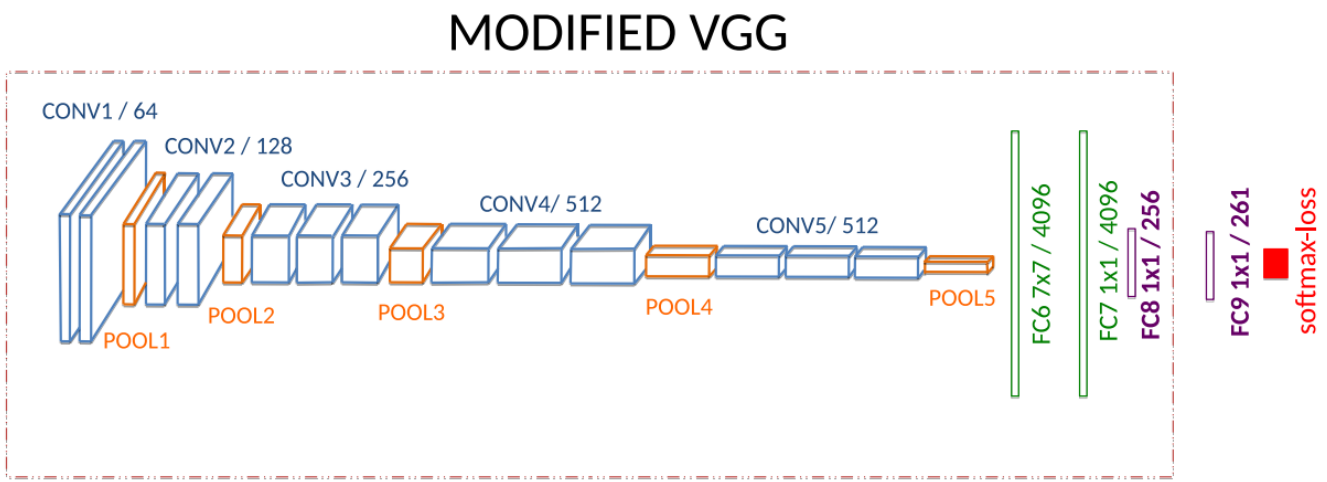

Adapted from [Luz et al., 2017].

CNN models training

- Transfer learning from the face domain (VGGFace) with fine-tuning (do not freezing any weights).
- Data augmentation - rotation.
- 30 epochs: 10 with $lr = 0.001$ and 20 with $lr = 0.0005$.
- SGD optimizer;
- Feature extractor training - SoftMax (identification)

Data Augmentation

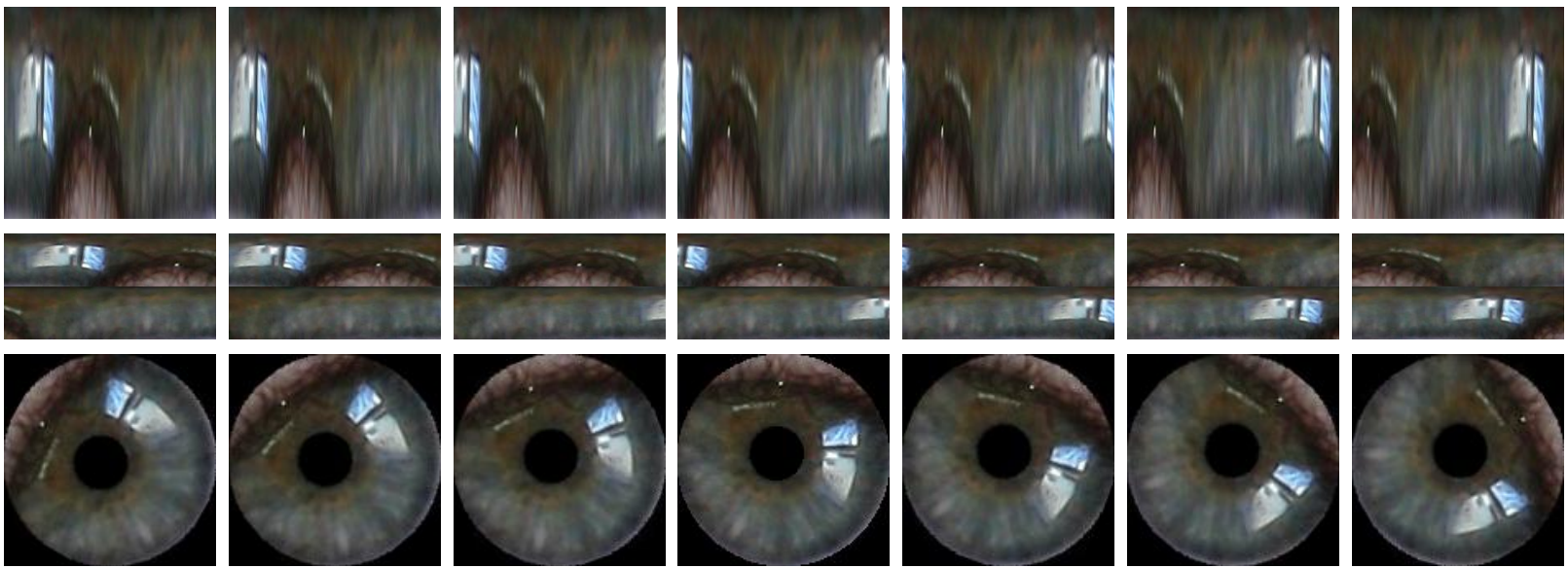

(-60) (-40) (-20) (original) (20) (40) (60)

Dataset

- NICE.II official contest database and protocol:
  - Training: 1000 images from 171 classes;
  - Testing: 1000 images from 150 classes;

Protocol and Matching

- Verification protocol (open world):
  - All against all:
  - 4,634 intra-class pairs;
  - 494,866 inter-class pairs;
- Metrics:
  - EER (Equal Error Rate): FAR = FRR;
  - Decidability: how well separated are intra- and inter-classes;
- Cosine distance metric;

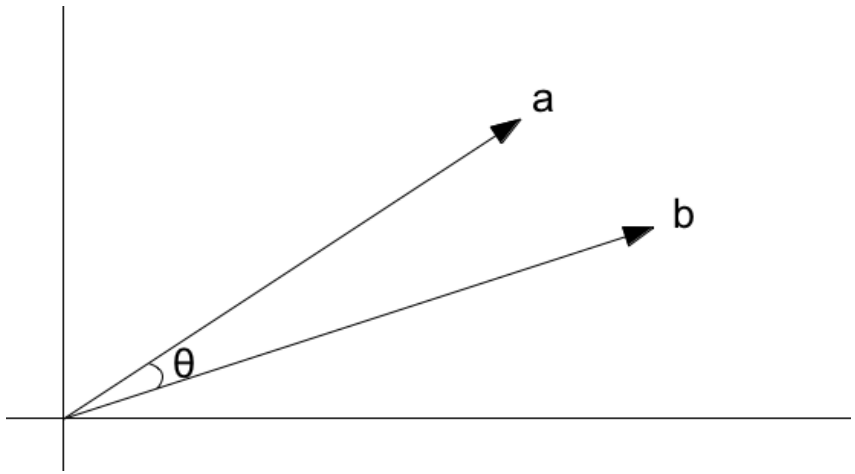

Experiments Analysis

- CNN models: VGG16 and ResNet50;
- Normalization: 8:1, 4:2 and Non-Norm;
- Data Augmentation;
- Segmentation;
- Delineation;
- 30 repetitions;
- T-test for statistical difference;

Data Augmentation

Network	Norm.	DA	EER (%)	Decidability
VGG16	8 : 1		26.19 ± 1.95	1.3140 ± 0.1246
VGG16	8 : 1	✓	23.63 ± 1.33	1.4712 ± 0.0881
ResNet-50	8 : 1		24.38 ± 1.41	1.4297 ± 0.0916
ResNet-50	8 : 1	✓	19.18 ± 0.75	1.7988 ± 0.0552
VGG16	4 : 2		24.77 ± 1.42	1.4127 ± 0.1001
VGG16	4 : 2	✓	18.74 ± 0.89	1.8527 ± 0.0712
ResNet-50	4 : 2		22.78 ± 1.22	1.5307 ± 0.0853
ResNet-50	4 : 2	✓	17.11 ± 0.53	1.9822 ± 0.0482
VGG16	Non-Norm		23.32 ± 1.10	1.4891 ± 0.0740
VGG16	**Non-Norm**	✓	$\mathbf{17.49 \pm 0.90}$	$\mathbf{1.9529 \pm 0.0760}$
ResNet-50	Non-Norm		21.51 ± 0.97	1.6119 ± 0.0677
ResNet-50	**Non-Norm**	✓	$\mathbf{13.98 \pm 0.55}$	$\mathbf{2.2480 \pm 0.0528}$

*white rows represent that there is statistical difference between: Models, Normalization and DA.

Segmentation for noise removal

Network	Norm.	Seg.	EER (%)	Decidability
VGG16	8 : 1	✓	22.58 ± 1.07	1.5437 ± 0.0697
VGG16	8 : 1		23.63 ± 1.33	1.4712 ± 0.0881
ResNet-50	8 : 1	✓	20.68 ± 1.39	1.6801 ± 0.1071
ResNet-50	8 : 1		19.18 ± 0.75	1.7988 ± 0.0552
VGG16	4 : 2	✓	18.00 ± 0.93	1.9055 ± 0.0750
VGG16	4 : 2		18.74 ± 0.89	1.8527 ± 0.0712
ResNet-50	4 : 2	✓	17.44 ± 0.85	1.9450 ± 0.0803
ResNet-50	4 : 2		17.11 ± 0.53	1.9822 ± 0.0482
VGG16	Non-Norm	✓	$\mathbf{17.48 \pm 0.68}$	1.9439 ± 0.0589
VGG16	Non-Norm		17.49 ± 0.90	1.9529 ± 0.0760
ResNet-50	Non-Norm	✓	14.89 ± 0.78	2.1781 ± 0.0794
ResNet-50	**Non-Norm**		$\mathbf{13.98 \pm 0.55}$	$\mathbf{2.2480 \pm 0.0528}$

*painted rows represent that there is no statistical difference

Delineation

Delineated

Non-delineated
(Bounding box)

Method	Delineated	EER (%)	Decidability
VGG16	✓	17.49 ± 0.90	1.9529 ± 0.0760
VGG16		17.52 ± 0.98	1.9652 ± 0.0790
Resnet-50	✓	13.98 ± 0.55	2.2480 ± 0.0528
Resnet-50		14.26 ± 0.47	2.2304 ± 0.0542

The state of the art comparison (Unpublished Results)

Results on the NICE.II contest dataset.

Method	EER (%)	Decidability
Wang et al.[Wang et al., 2012]	19.00	1.8213
Silva et al.[Silva et al., 2018] (Best Model)	14.56	2.2200
Proposed ResNet-50	**13.98**	**2.2480**
Proposed ResNet-50 ensemble (5 models)	9.53	2.8132
Proposed ResNet-50 ensemble (10 models)	9.27	2.8538
Proposed ResNet-50 ensemble (20 models)	9.21	2.8643
Proposed ResNet-50 ensemble (30 models)	9.15	2.8725

Conclusion

- Data Augmentation by rotation significantly improved the results;
- Non-normalized iris achieved a better result;
- ResNet-50 reported better result than VGG16;
- Delineated and Non-delineated images reported no statistical difference.

Future work - Other databases

Database	Spectrum	Classes/Images	Resolution
CASIA-Lamp	NIR	819/16212	640×480
CASIA-Thousand	NIR	2000/20000	640×480
UbirisV2	VIS	522/11102	400×300
MICHE DB	VIS(3 sensors)	184/3732	2322×4128 to 640×480
CSIP	VIS(10 sensors)	100/2004	3264×2448 to 640×480
VISOB	VIS(3 sensors)	1100/158136	240×160
MobBio	VIS	210/1680	300×200

Thank you!

e-mail: lazjunior@inf.ufpr.br

Bibliography I


Daugman, J. (1993).
High confidence visual recognition of persons by a test of statistical independence.
IEEE Transactions on Pattern Analysis and Machine Intelligence, 15(11):1148–1161.


Luz, E., Moreira, G., Junior, L. A. Z., and Menotti, D. (2017).
Deep periocular representation aiming video surveillance.
Pattern Recognition Letters.


Proença, H. and Alexandre, L. A. (2012).
Toward covert iris biometric recognition: Experimental results from the NICE contests.
IEEE Transactions on Information Forensics and Security, 7(2):798–808.

Bibliography II


Silva, P., Luz, E., Zanlorensi, L. A., Menotti, D., and Moreira, G. (2018).
Multimodal feature level fusion based on particle swarm optimization with deep transfer learning.
Research Gate.


Tan, T., He, Z., and Sun, Z. (2010).
Efficient and robust segmentation of noisy iris images for non-cooperative iris recognition.
Image and Vision Computing, 28(2):223–230.


Wang, Q., Zhang, X., Li, M., Dong, X., Zhou, Q., and Yin, Y. (2012).
Adaboost and multi-orientation 2D Gabor-based noisy iris recognition.
Pattern Recognition Letters, 33(8):978–983.